PHYSICAL REVIEW B VOLUME 18, NUMBER 7 1 OCTOBER 1978

Phonon heat transport and Knudsen's minimum in liquid helium at low temperatures

David Benin* and Humphrey J. Maris
Department of Physics, Brown University, Providence, Rhode Island 02912
(Received 27 December 1977)

The flow of heat in liquid ^{4}He at temperatures below 0.6°K is considered. Calculations are carried out for the specific cases of heat flow along a tube and flow down the channel between two parallel plates. It is assumed that the mean free path $\Lambda_\parallel$ for small-angle collisions between phonons is much less than the tube diameter or the spacing between the plates, but the calculations are valid for arbitrary values of the mean free path $\Lambda_\perp$ for large-angle collisions. For small $\Lambda_\perp$ the results are equivalent to the predictions of the Navier-Stokes equation with corrections for first- and second-order slip at the boundaries. For large $\Lambda_\perp$ the heat flow is close to the value given by Casimir's formula. At intermediate values of $\Lambda_\perp$ an effect similar to Knudsen's minimum is predicted by the theory. The calculations are compared briefly with the experimental results of Whitworth.

I. INTRODUCTION

At temperatures below about 0.6 °K the excitations in superfluid helium are almost exclusively long-wavelength phonons. These excitations form a low-density nearly ideal gas, which is the normal fluid of the Landau-Tisza two-fluid model.[1] The number density of this gas is the phonon number density, which varies as T^3 (T is the absolute temperature); the mass density, or normal-fluid density, varies as T^4. The phonons in the gas have a finite mean free path because of anharmonic interactions with other phonons and may also be scattered at the boundaries of the liquid. The gas has interesting hydrodynamic properties[2] that come about in the following way. It can be shown that because energy and momentum must be conserved in collisions between phonons nearly all collisions are of small angle (typically 5° or 10°). The effective large-angle scattering rate arises principally from repeated small-angle scattering processes. It is found that the large-angle scattering time $\tau_\perp$ is typically 10^4 times the small-angle scattering time $\tau_\parallel$. This means that after the gas has been disturbed from equilibrium, phonons with momenta in any given direction will rapidly come to equilibrium with each other, whereas groups of phonons with widely differing propagation directions will take a long time to equilibrate. Hence, for many problems which involve time scales long compared to $\tau_\parallel$ (or equivalently length scales long compared to the mean phonon velocity $\langle v\rangle$ times $\tau_\parallel$), one may describe the phonon gas by a local temperature $T(\vec{r},\hat{p})$ that depends on position $\vec{r}$ in real space and on the direction $\hat{p}$ in phonon momentum space.

It is possible to derive hydrodynamic equations that govern the rate of change of $T(\vec{r},\hat{p})$. The solution of these equations has been obtained in several cases of interest, and we mention two of these. (i) It has been shown[3] that, in addition to ordinary second sound, there are several other waves that can propagate through the gas, with more complicated oscillations of the phonon distribution function. (ii) Saslow[4] has found that when heat flows out from a solid boundary into superfluid helium a temperature gradient should be set up in the liquid layer near the solid. This gradient should decay roughly exponentially with distance from the surface and should be significant out to a distance of the order of the large-angle scattering mean free path

$$\Lambda_\perp \approx \langle v\rangle \tau_\perp . \tag{1}$$

We will define $\Lambda_\perp$ more precisely later on. As far as we know, there are no experiments to date that provide definite confirmation of these hydrodynamic effects.

In this paper we make some further calculations based on the hydrodynamic equations. The particular problem that we consider is the flow of the phonon gas along a tube or between two plates when the driving force is a temperature gradient. This is an interesting problem because the experiments required to compare with the theory are considerably simpler than the experiments needed to verify the two predictions mentioned above. In addition some experimental data taken by Whitworth[5] are already available with which to make comparisons.

As a preliminary to carrying out detailed calculations of the heat flow, we consider the flow of heat along a tube of radius R in two limiting cases. (a) Let R be so small that

$$R \ll \Lambda_\parallel , \tag{2}$$

where $\Lambda_\parallel$ is the small-angle collision mean free path. The problem is then exactly the same as

the boundary-scattering-limited heat flow in a dielectric solid. The heat flow along the tube must therefore be given by Casimir's formula,[6] i.e.,

$$\dot{Q} = \pi R^2 K_{\text{Casimir}} \frac{dT}{dx}, \tag{3}$$

where dT/dx is the temperature gradient along the tube, whose axis is taken to be parallel to the x direction, and

$$K_{\text{Casimir}} = \tfrac{1}{3} C\langle v\rangle 2R . \tag{4}$$

C is the specific heat of the phonons and Eq. (4) is really just the kinetic formula with an effective mean free path

$$\Lambda_{\text{eff}} = 2R . \tag{5}$$

(b) Let R be such that

$$R \gg \Lambda_{\perp} . \tag{6}$$

In this case the phonons behave like a gas with viscosity η (the normal-fluid viscosity). The gas is driven through the tube by the gradient in fountain pressure.[1] This is given by

$$\frac{dP}{dx} = S\frac{dT}{dx}, \tag{7}$$

where S is the entropy per unit volume. The volume of phonon gas flowing through the tube per unit time is then given by Poiseuille's formula

$$\dot{V} = \frac{\pi R^4}{8\eta}\frac{dP}{dx} . \tag{8}$$

The entropy flow rate $\dot{S}$ is $S\dot{V}$ and so the heat flow is

$$\dot{Q} = T\dot{S} = \frac{\pi R^4 S^2 T}{8\eta}\frac{dT}{dx} . \tag{9}$$

For a tube with radius R such that

$$\Lambda_{\perp} > R > \Lambda_{\parallel} ,$$

there exists no simple theory of the heat flow. The full hydrodynamic equations for the phonon gas must then be used. Using the notation of Whitworth[5] we can express the problem in the following form. Equation (3) can be written

$$\dot{Q} = \tfrac{1}{3}\pi R^2 C\langle v\rangle \Lambda_{\text{eff}} \frac{dT}{dx} , \tag{10}$$

where we have replaced $2R$ by the mean free path Λ_{eff}. Whitworth uses this equation to *define* Λ_{eff} in all situations regardless of the tube diameter. He then defines a quantity

$$y \equiv \Lambda_{\text{eff}}/2R . \tag{11}$$

For $R \ll \Lambda_{\parallel}$, y is equal to 1, and in the opposite limit of $R \gg \Lambda_{\perp}$, it follows from Eq. (9) that

$$y = 3RS^2T/16\eta C\langle v\rangle . \tag{12}$$

We now choose to define the large-angle phonon mean free path $\Lambda_{\perp}$ by[7]

$$\eta = \tfrac{1}{5}\rho_n\langle v\rangle\Lambda_{\perp} , \tag{13}$$

where ρ_n is the normal-fluid density. For a phonon gas in which all phonons have the same velocity it is true that

$$S^2T/\rho_n\langle v^2\rangle C = \tfrac{1}{3} . \tag{14}$$

Thus

$$y = 5R/16\Lambda_{\perp} \tag{15}$$

for $R \gg \Lambda_{\perp}$. Hence, the limiting values of y are as shown schematically by the solid lines in Fig. 1.

An interesting feature of Whitworth's results is that a shallow minimum in y is found at around

$$R/\Lambda_{\perp} = 0.44 \pm 0.07 . \tag{16}$$

This is shown quantitatively by the dashed line in Fig. 1. The value of y at the minimum is slightly less than 1. The same effect has been observed in the flow or ordinary gases through tubes by Knudsen[8] in 1909, who found for several different gases at room temperature a minimum at

$$R/\Lambda_{\perp} \approx 0.12 \text{ to } 0.13 . \tag{17}$$

No simple explanation of Knudsen's minimum has been given. Thus it is interesting to ask whether the difference in the positions of the Knudsen minimum in superfluid helium and in gases is a consequence of the peculiar hydrodynamics of helium. We will be able to show that this is indeed the case. Our calculation, however, gives a minimum at $R/\Lambda_{\perp} = 0.20$, intermediate between (16) and (17). While this is not in agreement with Whitworth's conclusions, neither is it inconsistent with his experimental data; we shall discuss this question in Sec. V.

Whitworth's data have been previously analyzed theoretically by Simons,[9] who was able to show that a flow minimum in a phonon system could be deduced from a Boltzmann equation approach. In Simon's approach all phonon-phonon scattering is represented by a single mean free path. As mentioned in our introductory discussion, it is now believed that a single mean free path theory is

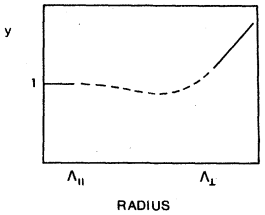

FIG. 1. Qualitative dependence of y upon tube radius R.

not an adequate quantitative description of the hydrodynamics of phonons in liquid helium.

II. GENERAL CONSIDERATIONS REGARDING HEAT FLOW

For a review of the hydrodynamics of phonons in superfluid ^{4}He, see Refs. 1 and 2. We shall treat heat flow along a tube or down the channel between two parallel plates under the conditions $\Lambda_{\parallel} \ll R$ (in the plane-geometry case R is the spacing between plates). The relevant lengths in the problem are then R and $\Lambda_\perp$, and on the scale of either of these there are many small-angle collisions. The distribution function $N(\vec{r},\vec{p})$ for phonons in the liquid may then be specified by a temperature $T(\vec{r},\hat{p})$ as described above, and we assume

$$N(\vec{r},\vec{p}) = 1/\{\exp[\epsilon_p/k_B T(\vec{r},\hat{p})] - 1\}, \tag{18}$$

where ϵ_p is the energy of a phonon of momentum $\vec{p}$. A kinetic equation for $T(\vec{r},\hat{p})$ may be derived from the linearized phonon Boltzmann equation; in the general case of a time dependence of T this equation is

$$\left(\frac{\partial}{\partial t} + \vec{v}\cdot\vec{\nabla}\right) T(\vec{r},t,\hat{p}) = -\sum_{lm} \frac{1}{\tau_l} Y_{lm}(\hat{p})(Y_{lm},T). \tag{19}$$

Here $\vec{v} = \langle v\rangle \hat{p}$ with $\langle v\rangle$ a thermal average of the phonon group velocity, the Y_{lm} are spherical harmonics in the angular variables θ_p, ϕ_p of $\hat{p}$, and

$$(Y_{lm},T) \equiv \int\int d\cos\theta_p\, d\phi_p Y^*_{lm}(\hat{p}) T(\vec{r},t,\hat{p}).$$

The times τ_l are the relaxation times for the various l components in the angular variation of T in $\hat{p}$ space. The relaxation occurs because of collisions between phonons. If T is independent of direction in $\hat{p}$ space ($l=0, m=0$), one has complete (local) thermal equilibrium and collisions can cause no change in the distribution. Thus $1/\tau_0$ must be zero. Similarly the $l=1$, $m=0$ component of T represents a simple drift of the phonon gas in the polar direction, and this too is unaffected by collisions, which conserve phonon momentum. Hence $1/\tau_1$ is also zero. A simple expression for the remaining relaxation times can only be given if the collision angle is very small. In this case it can be shown that[2,10]

$$1/\tau_l = (l-1)l(l+1)(l+2)(1/24\tau_2). \tag{20}$$

Equation (20) in fact becomes inaccurate for large l; it is a reasonable approximation only if $l\alpha \ll 1$, where α is the mean angle between colliding phonons. We shall later consider the effect on our results of using a more accurate expression for τ_l.

In addition it has been shown that the effective large-angle mean free path $\Lambda_\perp$, related to the phonon viscosity by Eq. (13), is simply

$$\Lambda_\perp = \langle v\rangle \tau_2. \tag{21}$$

In the heat-flow problems we shall treat we take the flow to be in the x direction, along the axis of a cylindrical tube or parallel to the walls down the channel between two infinite parallel plates. We then seek time-independent solutions of (19) in which the walls provide a constant temperature gradient dT/dx. Thus we put

$$T(\vec{r},\hat{p}) = T_0 + [x - \chi(\vec{\rho},\hat{p})]\frac{dT}{dx}, \tag{22}$$

where $\vec{\rho}$ is a two-dimensional vector denoting position in the cross-sectional plane perpendicular to the flow, and T_0 is the wall temperature at $x = 0$. Equation (19) than becomes

$$\hat{p}_\perp \cdot \vec{\nabla}_{\vec{\rho}} \chi(\vec{\rho},\hat{p}) = -\sum_{lm} \frac{1}{\Lambda_l} Y_{lm}(\hat{p})(Y_{lm},\chi) + \hat{p}_x, \tag{23}$$

where $\hat{p}_\perp$ is the component of the unit vector $\hat{p}$ in the cross-sectional plane, and $\Lambda_l = \langle v\rangle \tau_l$. [We shall henceforth write Λ_2 instead of $\Lambda_\perp$—cf. Eq. (21).] Equation (23) is to be solved for χ, subject to a boundary condition expressing how phonons scatter from the walls. We shall treat only the model of purely diffuse boundary scattering, in which phonons returning after being scattered at the wall have a distribution identical to that radiated by a black body. For those phonons, the effective temperature is thus independent of propagation direction and is equal to the local wall temperature $T_0 + x(dT/dx)$. Thus

$$\chi(\vec{\rho}',\hat{p}) = 0 \quad \text{for } \hat{p}\cdot\hat{n}' > 0 \tag{24}$$

holds for each point $\vec{\rho}'$ on the walls, with $\hat{n}'$ the inward normal to the wall at $\vec{\rho}'$.

Our procedure shall be to solve Eq. (23) with (24) for the two geometries to evaluate the energy flux in the x direction, $q_x(\vec{\rho})$ at the point $\vec{\rho}$ in the cross section. This is

$$q_x(\vec{\rho}) = \frac{1}{(2\pi\hbar)^3}\int d^3p\, \epsilon_p v_x N(\vec{r},\vec{p});$$

using Eqs. (18) and (22) this works out to linear order in dT/dx to be

$$q_x(\vec{\rho}) = -\tfrac{1}{3} C\langle v\rangle \Lambda_{\text{eff}}(\vec{\rho})\frac{dT}{dx}, \tag{25a}$$

with

$$\Lambda_{\text{eff}}(\vec{\rho}) = \frac{3}{4\pi}\int\int d\cos\theta_p\, d\phi_p \hat{p}_x \chi(\vec{\rho},\hat{p}). \tag{25b}$$

Integrating $q_x(\vec{\rho})$ over the cross section, the total heat flow may be written in the form of Eq. (10)

above [with the cross-sectional area A replacing πR^2 in (10)] and with the heat flow mean free path in Eq. (10) given by the average

$$\Lambda_{eff}=\frac{1}{A}\int d^2\vec{\rho}\,\Lambda_{eff}(\vec{\rho})\,. \tag{25c}$$

Before turning to specific solutions it is useful to list some features common to our methods of solution in both geometries. The inhomogeneous term $\hat{p}_x$ in Eq. (23) is odd under reflection of $\hat{p}$ in the cross-sectional plane. Since both of the other operators in Eq. (23) conserve the parity of $\chi(\vec{\rho},\hat{p})$ under this reflection, χ must be an odd function of p_x, as is consistent with the boundary condition (24).

In both geometries to be considered one can find particular solutions to the inhomogeneous Eq. (23) without difficulty; these shall be presented later. The complementary solution of the homogeneous version of (23) will be constructed in the following way. We first seek elementary "planar" solutions $\psi(\vec{\rho},\hat{p})$, each of which depends upon a single Cartesian component of the cross-sectional position coordinate $\vec{\rho}$. We call this Cartesian component the z direction. These solutions are required to satisfy

$$\hat{p}_z\frac{\partial}{\partial z}\psi(z,\hat{p})=-\sum\frac{1}{\Lambda_l}Y_{lm}(\hat{p})(Y_{lm},\psi)\,. \tag{26}$$

We use a coordinate system for $\hat{p}$ with polar axis along the z direction. Then $\hat{p}_z=\cos\theta_p$, so different m values are not coupled in (26) and solutions of definite helicity m exist. As discussed above though, we need solutions that are odd functions of $\hat{p}_x=\sin\theta_p\cos\phi_p$. This requires that spherical harmonics appear in the solution in the combinations

$$[Y_{lm}(\hat{p})+(-1)^mY_{l\bar{m}}(\hat{p})]\propto P_{lm}(\cos\theta_p)\cos(m\phi_p),\quad m=1,3,5,\ldots\,.$$

We thus look for odd-m solutions, in the form

$$\psi_m(z,\hat{p})=e^{-kz}\sum_l\frac{2l+1}{2}\frac{(l-m)!}{(l+m)!}D_{lm}\times P_{lm}(\cos\theta_p)\cos(m\phi_p)\,. \tag{27}$$

Substituting (27) into (26) and using

$$\cos\theta P_{lm}=\frac{l+1-m}{2l+1}P_{l+1,m}+\frac{l+m}{2l+1}P_{l-1,m}\,,$$

one obtains the set of conditions

$$(l+1-m)D_{l+1,m}+(l+m)D_{l-1,m}-\frac{2l+1}{k\Lambda_l}D_{lm}=0\,, \tag{28}$$

which holds for $l\geq m$, with $D_{m-1,m}\equiv 0$. Thus, for each m, there is a spectrum of allowed values of k, which is to be found by equating the determinant of the coefficients of the D_{lm} in (28) with zero. This is, strictly, an infinite tridiagonal determinant. However, because the terms along the principal diagonal contain $1/\Lambda_l$ and these increase rapidly with increasing l, one can obtain a good approximation to those solutions for k which are fairly small by truncating the determinant at some maximum value of l. Alternately one can recurse (28) upwards in l and set $D_{l+1,m}=0$ for some maximum l; this is an entirely equivalent procedure, since the determinant is tridiagonal. Results obtained for the k's in this way are given in Table I, where they are expressed in units of $1/\Lambda_2$. It is easily shown from (26) or (28) that roots for k always occur in ± pairs; only the positive member of each pair is entered in Table I. We denote the ith positive root by k_{mi}, the associated D_{lm} coefficients by D_{lmi}, and the solution $\psi_m(\vec{\rho},\hat{p})$ by $\psi_{mi}(\vec{\rho},\hat{p})$. We arbitrarily choose D_{mmi} equal to 1 for all i.

TABLE I. Decay constants k_{mi} for some of the low-order modes. The actual values are the numbers given in the table multiplied by Λ_2^{-1}.

	$m=1$	3	5	7	9
$i=1$	16.6	23.5	145	497	1270
2	92.4	106	384	1020	2250
3	301	324	866	1930	
4	746	780	1720		
5	1560	1610			

We note in passing that Eqs. (27) and (28) also apply to the even-m solutions of (26), including the $m=0$ case given preliminary consideration by Saslow.[4]

Because of energy and momentum conservation, there are additional solutions of Eq. (26) which are not of the exponential form (27). One can easily verify that because $1/\Lambda_0$ and $1/\Lambda_1$ are zero, the determinant of coefficients of the D_{lm} in Eq. (28) has a twofold degenerate root $k=0$ in both the $m=0$ and $m=1$ cases, and in no others; thus there are four nonexponential solutions, two $m=0$ and two $m=1$. The two $m=1$ solutions of interest here are

$$\psi'(z,\hat{p})=\hat{p}_x\,, \tag{29}$$

$$\psi''(z,\hat{p})=z\hat{p}_x-\Lambda_2\hat{p}_x\hat{p}_z\,. \tag{30}$$

The first solution describes a simple uniform flow of the phonon gas in the x direction, and the second a shear flow in the x direction, with a constant flow-velocity gradient in the z direction.

For heat flow between parallel plates each of these solutions has the desired planar symmetry

if the z direction is the normal to the plates. The problem reduces to choosing a suitable linear combination of these solutions to satisfy the boundary conditions. For flow along a tube it is first necessary to generate solutions of cylindrical symmetry from the elementary planar solutions. This will be performed in Sec. III.

III. FLOW IN A TUBE

We now consider phonon flow along a tube of radius R. For this problem it is most convenient to describe the phonon distribution function by angle variables θ_p' and ϕ_p' which use the tube axis x as the polar axis. A particular solution of Eq. (23) can then be shown to be

$$\chi_{\text{part}} = -\frac{5}{4\Lambda_2}(\rho^2 - R^2)P_{10}(\cos\theta_p') + \tfrac{5}{6}\rho P_{21}(\cos\theta_p')\cos(\phi_p' - \theta) + \Lambda_3 P_{30}(\cos\theta_p'), \tag{31}$$

where ρ is the magnitude of the vector $\vec{\rho}$ and the origin of $\vec{\rho}$ has been chosen to be at the axis of the tube. θ is the angle between $\vec{\rho}$ and the y axis as shown in Fig. 2. This particular solution has been chosen to give the full heat flow in the Poiseuille flow limit discussed in Sec. I.[11] This will be shown explicitly in Sec. V.

To construct the complementary solutions we begin with a planar solution of the form of Eq. (27). This solution is then rotated by an angle α around the x axis, as shown in Fig. 2. Let the new solution be $\psi_{mi}(\alpha)$. We now form a linear combination of such solutions by integrating over α to get

$$\psi_{mi,\text{cyl}} = (2\pi)^{-1}\int_0^{2\pi}\psi_{mi}(\alpha)\,d\alpha\,. \tag{32}$$

$\psi_{mi,\text{cyl}}$ can be expressed as a sum of spherical harmonics of θ_p' and ϕ_p' by using the Wigner rotation coefficients. The result of the integral in Eq. (32) can then be written

$$\psi_{mi,\text{cyl}} = \sum_{lm'} B_{lm'i}(\rho)P_{lm'}(\cos\theta_p')\cos m'(\phi_p' - \theta) \tag{33}$$

where

$$B_{lm'i}(\rho) = \frac{(2l+1)}{2}\left(\frac{(l-m)!\,(l-m')!}{(l+m)!\,(l+m')!}\right)^{1/2} \times[1+(-1)^{l+m'}]D_{lmi}d^l_{m'm}I_{m'}(k_{mi}\rho)\,, \tag{34}$$

$$d^l_{m'm} = \sum_s \frac{(-1)^s[(l+m)!\,(l-m)!\,(l+m')!\,(l-m')!\,]^{1/2}}{(l-m'-s)!\,(l+m-s)!\,(s+m'-m)!\,s!}\,. \tag{35}$$

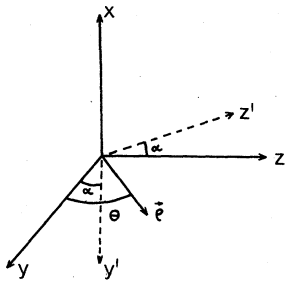

FIG. 2. Coordinate systems used to form cylindrical symmetry solutions from planar solutions.

$I_{m'}$ is the modified Bessel function. The sum over s in Eq. (35) is over all integer values such that the arguments of all of the factorials are non-negative. The solution (33) has cylindrical symmetry since it is clearly invariant with respect to rotation about the x axis. Thus, for example, the distribution depends on $(\phi_p' - \theta)$, but not on ϕ_p' and θ separately. A complementary solution can also be constructed from the solution (29) in the same manner. This gives

$$\psi'_{\text{cyl}} = \cos\theta_p'. \tag{36}$$

This solution is independent of position in real space and represents a homogeneous drift of the phonon gas in the direction along the tube. The other special solution ψ'' given by Eq. (30) vanishes when rotated through all angles.

We believe these are the only complementary solutions that have cylindrical symmetry and are free of sources. Solutions also exist that contain the modified Bessel functions K_m, but these are singular at $\rho = 0$ and thus not source free.

The probelm now is to construct a linear combination of the particular solution with the complementary solutions such that the boundary condition Eq. (24) at the tube wall is satisfied. In the new coordinate system this boundary condition is

$$\chi(R, \theta, \theta_p', \phi_p') = 0 \tag{37}$$

for

$$\tfrac{1}{2}\pi \leq \phi_p' - \theta \leq \tfrac{3}{2}\pi\,,$$

which describes phonons leaving the wall of the tube.

We have solved this problem numerically by the following method. We first selected 15 of the complementary solutions. These 15 included the solution (36), together with the 14 solutions produced by rotation of all plane waves that satisfied the conditions

$$m \leq 6\,, \qquad k_{mi} < 2700/\Lambda_2\,. \tag{38}$$

We then formed the solution

$$\chi = \chi_{\text{part}} + A_0 \psi'_{\text{cyl}} + \sum_{\alpha=1}^{14} A_\alpha \psi_\alpha \,, \tag{39}$$

where the rotated plane solutions are denoted by ψ_α. We then constructed the quantity

$$F = \int_{-1}^{1} d\cos\theta'_p \int_{\pi/2}^{3\pi/2} d\phi'_p \chi^2(R, 0, \theta'_p, \phi'_p) \,. \tag{40}$$

If the boundary condition were satisfied exactly, F would be zero. The coefficients A_α were adjusted to minimize F. A measure of the success achieved in meeting the boundary condition is provided by the ratio

$$\beta \equiv F/F_0 \,, \tag{41}$$

where F_0 is the same integral as F but with the ϕ'_p integration extended from 0 to 2π. β was generally between 0.01 and 0.02.

In Fig. 3 we show the results of the calculation for a range of values of the quantity R/Λ_2. Figure 4 shows results for the flow velocity of the phonon gas as a function of position in the tube. We shall discuss the interpretation of these results in detail in Sec. V.

These results change only slightly when more complementary solutions are included. For example, we have investigated the result obtained by including all of the 20 complementary solutions with $m \leq 9$ and $k_{mi} < 2700/\Lambda_2$. This leads to a reduction in β by about a factor of 2, but changes Λ_{eff} by less than 0.2%. The calculations become

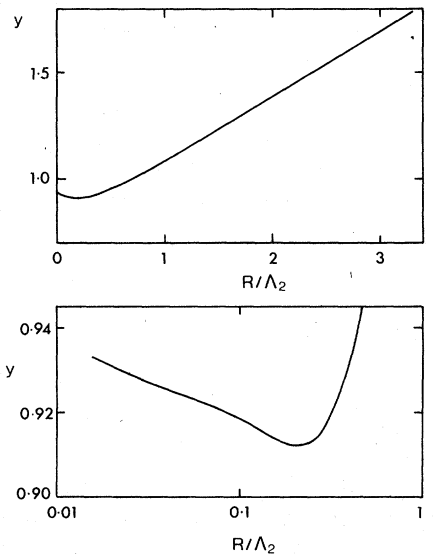

FIG. 3. Results of calculations of the effective mean free path Λ_{eff} for heat flow along a tube of radius R. The results are expressed in terms of the dimensionless quantity $y = \Lambda_{\text{eff}}/2R$.

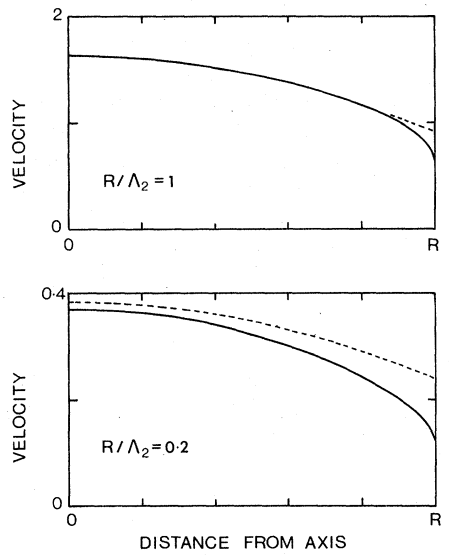

FIG. 4. Flow velocity (solid curves) of the phonon gas as a function of distance from the tube axis for two tubes of different radius. The dashed curves show the velocity as calculated from the Navier-Stokes equation with a slip correction. The units of velocity are arbitrary, but correspond to the same temperature gradient for each tube.

difficult numerically when R/Λ_2 is small since the amplitude of the various complementary solutions become large, and the minimization of F leads to an expression for the A_α that involves a nearly singular matrix. Thus we are unable to obtain accurate results for R/Λ_2 less than about 0.02.

The effect on these results of using a more accurate expression for τ_i (see, for example, Ref. 3) was found to be very small.

IV. FLOW BETWEEN PLANE WALLS

Our motivation for studying heat flow between parallel plates is primarily theoretical. For plane geometry the solution of Eqs. (23) and (24) can be carried farther analytically than in cylindrical geometry, with the boundary conditions treated in a different manner than the variational approach of Sec. III. Moreover, in one respect our plane calculation serves as a direct check on the accuracy of the results for cylinders—this is in the value of a first-order slip coefficient, to be discussed in Sec. V, which should be independent of geometry, and for which the two calculations are in fact in good agreement.

A. Particular solution

We employ the notation of Sec. II and consider heat flow in the x direction along a channel of

width W. The two infinite plane walls are at $z=0$ and $z=W$. As discussed in Sec. II, we need consider only azimuthal variations in the temperature distribution $\chi(z,\hat{p})$ which vary like $\cos(m\phi_p)$ with m odd; in fact only $m=1$ is involved since the inhomogeneous term in Eq. (23) is $\hat{p}_x=\sin\theta_p\cos\phi_p$.

A particular solution of Eq. (23) is

$$\chi_{\text{part}}(z,\hat{p})=\left(\frac{5}{2\Lambda_2}z(W-z)P_{11}(\cos\theta_p)+\tfrac{5}{3}(z-\tfrac{1}{2}W)P_{21}(\cos\theta_p)-\tfrac{2}{3}\Lambda_3P_{31}(\cos\theta_p)\right)\cos\phi_p\,. \tag{42}$$

As with the particular solution in cylindrical geometry, Eq. (31), here too the above particular solution has been chosen to give the full heat flow in the Poiseuille flow limit. This will be discussed explicitly in Sec. V. To this must be added a complementary solution $\chi_c(z,\hat{p})$ of the homogeneous equation, which, in view of the boundary condition Eq. (24), must satisfy

$$\chi_c(0,\hat{p})=[\tfrac{5}{6}WP_{21}(\cos\theta_p)+\tfrac{2}{3}\Lambda_3P_{31}(\cos\theta_p)]\cos\phi_p \quad \text{for } \cos\theta_p>0\,,$$

$$\chi_c(W,\hat{p})=[-\tfrac{5}{6}WP_{21}(\cos\theta_p)+\tfrac{2}{3}\Lambda_3P_{31}(\cos\theta_p)]\cos\phi_p \quad \text{for } \cos\theta_p<0\,.$$

Our method for determining χ_c involves two fundamental approximations which allow reduction to a half-space problem, and subsequent truncation of an expansion in the elementary solutions.

B. Half-space approximation

The complementary solution χ_c can, of course, be expanded in the elementary solutions $\psi(z,\hat{p})$ discussed in Sec. II. All but two of these elementary solutions decay or grow exponentially in z, like $e^{\pm k|z|}$. Thus each $\pm k$ pair of exponential elementary solutions contributes a spatial transient to χ_c, which is important only in a layer near each boundary of thickness $\sim 1/k$. As seen from Table I, each $1/k$ is small compared to the wide-angle mean free path Λ_2, so even when the spacing between walls is comparable to Λ_2 the spatial transients do not extend out very far from either wall into the flow channel. This circumstance allows us to approximate the complementary solution χ_c obeying parallel-plate boundary conditions by superposing two solutions obeying boundary conditions on a half-space. We shall proceed as follows. Suppose we can find a function $\Psi(z,\hat{p})$ satisfying Eq. (26) on a half-space $0\leq z<\infty$, with the same boundary condition as χ_c at $z=0$, i.e.,

$$\Psi(0,\hat{p})=(\tfrac{5}{6}WP_{21}+\tfrac{2}{3}\Lambda_3P_{31})\cos\phi_p,\quad \cos\theta_p>0$$

and with bounded asymptotic value $\Psi(\infty,\hat{p})$ as $z\to\infty$. Since Ψ is bounded, it is a superposition of only the exponentially decaying elementary solutions, plus the uniform solution ψ', Eq. (29). Ψ thus consists of spatial transients in a boundary layer near $z=0$, plus an asymptotic part. As argued above, the transients will be exponentially small at $z=W$, even for $W\sim\Lambda_2$. The asymptotic part $\Psi(\infty,\hat{p})$, which is the ψ' term in the superposition, is an even function of $\cos\theta_p$. Then the parallel-plates complementary solution, for $0\leq z\leq W$, is

$$\chi_c(z,\cos\theta_p,\cos\phi_p)=\Psi(z,\cos\theta_p,\cos\phi_p)+\Psi(W-z,-\cos\theta_p,\cos\phi_p)-\Psi(\infty,\cos\theta_p,\cos\phi_p)+O(e^{-|k|W})\,. \tag{43}$$

The first term on the right-hand side by itself satisfies the correct boundary condition at $z=0$, and the sum of the second and third terms is exponentially small there. A similar situation holds at $z=W$. In what follows we shall approximate χ_c by the first three terms on the right-hand side of Eq. (44), which should be valid even in the region $W\sim\Lambda_2$ where the Knudsen flow minimum occurs.

C. Expansion in elementary solutions

To compute $\Psi(z,\hat{p})$ we shall make use of some orthogonality properties of the elementary solutions $\psi(z,\hat{p})$ when integrated over the angular variables $\hat{p}$ at $z=0$. In the inner-product notation of Eq. (19), these properties are

(a) $(\psi_{mi}\cos\theta_p,\psi_{m'i})=0$ for $(m,i)\neq(m',i')$,

(b) $(\psi_{mi}\cos\theta_p,\psi')=(\cos\theta_p\psi_{mi},\psi'')=0$,

(c) $(\psi'\cos\theta_p,\psi')=(\cos\theta_p\psi'',\psi'')=0$,

(d) $(\psi'\cos\theta_p,\psi'')=-\frac{4}{15}\pi\Lambda_2$,

with all ψ's at $z=0$. These may be proven in the usual manner from Eq. (26) or by direct integration. Relation (a) applies to any two solutions whose decay constants k are not the same, including the two members of a $\pm k$ pair. Relations (c) and (d), which assert that ψ' and ψ'' are orthogonal to themselves but not to each other, are the only unusual consequences of the non-positive-definite weight function $\cos\theta_p$.

These orthogonality relations allow one to determine expansion coefficients. If a function $f(z,\hat{p})$ has the expansion

$$f=\sum_{mi} A_{mi}\psi_{mi}+A'\psi'+A''\psi'', \tag{44}$$

then the coefficients are related to the boundary value $f(0,\hat{p})\equiv f_0(\hat{p})$ as follows:

$$A_{mi}=(\psi_{mi}\cos\theta_p,f_0)/(\psi_{mi}\cos\theta p,\psi_{mi}), \tag{45a}$$

$$A'=(\psi''\cos\theta_p,f_0)/(\psi''\cos\theta_p,\psi), \tag{45b}$$

$$A''=(\psi'\cos\theta_p,f_0)/(\psi'\cos\theta_p,\psi''), \tag{45c}$$

with all ψ's at $z=0$. In Eqs. 45(b) and 45(c), which projections determine which expansion coefficient is just the reverse of what one would normally expect, as a consequence of the "backwards" orthogonality relations (c) and (d) above.

The solution $\Psi(z,\hat{p})$ of the half-space problem above involves a superposition of $m=1$ exponentially decaying elementary solutions ψ_{1i}, and ψ':

$$\Psi(z,\hat{p})=\sum_i A_i\psi_{1i}(z,\hat{p})+A'\psi'(z,\hat{p}). \tag{46}$$

At the boundary $z=0$ we may also write

$$\Psi(0,\hat{p})\equiv\Psi_0(\hat{p})=\begin{cases}[\frac{5}{6}WP_{21}(\cos\theta_p)+\frac{2}{3}\Lambda_3 P_{31}(\cos\theta_p)]\cos\phi_p, & \cos\theta_p>0, \quad (47a)\\ \sum_i B_i\psi_{1i}(0,\hat{p})+B'\psi'(0,p), & \cos\theta_p<0. \quad (47b)\end{cases}$$

The B_i are coefficients in the expansion, over half the angular range, of just the incoming part of ψ_0 describing phonons incident on the wall at $z=0$. They are the same as the A_i in the full-angular-range expansion (46) if *all* the modes ψ_{1i} are retained, but only in that case, since in general it requires all the modes in the A_i expansion to exactly reproduce (47a) for the outgoing distribution. In what follows we shall truncate both the A_i and B_i expansions after a finite number of modes. Then (47b) is an *approximation* to the actual incoming distribution, and (46) a further approximation of the full-range expansion representing (47a) and the truncated (47b). In that case the A_i and B_i are not identical. A physical justification for this truncation will be given shortly.

The B_i are determined by requiring that Ψ_0 given by (47) be orthogonal, in the sense of Eqs. (45), to all exponentially growing solutions, and also to ψ', because of Eq. (45c). This results in the following set of inhomogeneous equations determining the B's:

$$\sum_{i'} M_{ii'}B_{i'}=\tfrac{5}{6}W\alpha_i+\tfrac{2}{3}\Lambda_3\beta_i, \tag{48a}$$

with

$$\alpha_i=\frac{12}{5}\sum_l D_{l1i}(-1)^l J_{l2}, \tag{48b}$$

$$\beta_i=\frac{24}{7}\sum_l D_{l1i}(-1)^l J_{l3}, \tag{48c}$$

$$M_{ii'}=\sum_{ll'} D_{l1i}D_{l'1i'}(-1)^{l'}J_{ll'}, \tag{48d}$$

and

$$J_{ll'}=\int_0^1 d(\cos\theta)P_{l1}(\cos\theta)P_{l'1}(\cos\theta)\cos\theta. \tag{48e}$$

These equations also determine the coefficient B' of the uniform flow mode if we extend the indices to include $i,i'=0$ and define $B'\equiv B_0$ and $D_{l10}\equiv\frac{4}{3}\delta_{l,1}$, so that ψ' in Eq. (29) may be written in the form of Eq. (27).

In actual practice we shall truncate this set after a finite number of modes with the smallest few k values. In a given approximation, the number of modes retained, their k values, and the coefficients D_{l1i} in their expansion Eq. (27) are all determined as in Sec. II, by truncating the $m=1$ determinant for the k's at a given maximum l.

This procedure may be thought of simply as a way of parametrizing a sequence of approximations to the incoming distribution at the boundary, Ψ_0 for $\cos\theta_p<0$. The truncation scheme is based on this idea: whatever the particular mixture of exponentially decaying modes with large k's necessary to guarantee that the outgoing distribution is given by Eq. (47a). Nevertheless for large enough k these rapidly decaying modes represent negligible disturbances in the phonon population in incoming directions $\cos\theta_p<0$, and thus do not contribute to (47b). Qualitatively one might expect this, on the following grounds. Modes which are rapidly attenuated in space must represent some combination of two features. These are (i) strong relaxation effects due to small-angle scattering, characterized by short mean free paths, and (ii) effects of wide-angle scattering on phonons moving nearly parallel to the boundary plane $z=0$, which thus do not get very far away from the plane before they relax via wide-angle scattering. The first effect requires rapid angular oscillations in the distribution function, so that scattering through just a small angle can have a surplus phonon fill in a deficit. For a disturbance which attenuates as one moves *outward* from the boundary, the

oscillations must be in outgoing directions only. The second effect requires that surplus phonons traveling nearly parallel to the boundary be coupled by wide-angle scattering to deficits more nearly perpendicular to the boundary. These deficits must be in *outgoing* near-perpendicular directions, in order that they too be rapidly attenuated in z, due to coupling via small-angle scattering to a nearby surplus of phonons, as in the first effect. Thus for either of features (i) or (ii) to be present, the distribution function should deviate from equilibrium primarily just for phonons going outward from the boundary plane. This line of reasoning seems fairly well confirmed in practice. For example, Fig. 5 shows the $\cos\theta_p$ dependence of the mode ψ_{1i} for the fifth smallest k value for $m=1, k_i=1558/\Lambda_2$. There are rapid oscillations for $\cos\theta_p>0$, a large peak of surplus phonons for directions roughly parallel to the boundary plane, and only a small disturbance over much of the incoming hemisphere $\cos\theta_p<0$. Thus, neglecting the contribution to the incoming distribution from this mode and others with similar behavior should make little difference.

The boundary distribution Ψ_0 is thus given by Eq. (47a) and the series of (47b), truncated in a given approximation. Equations (45a) and (45b), with this Ψ_0 in the inner products, then give the coefficients A_l in the full-range expansion Eq. (46); as discussed above, these are not exactly the same as the B_i since the half-range expansion for the incoming distribution has been truncated. With $A_0 \equiv A'$, we obtain

$$A_i = \left(\tfrac{5}{6} W a_i + \tfrac{2}{3}\Lambda_3 b_i + \sum_{i'} L_{ii'} B_{i'}\right)/N_i\,, \qquad (49)$$

with

$$a_i = \frac{12}{5}\sum_l D_{l1i} J_{l2}\,,$$

$$b_i = \frac{24}{7}\sum_l D_{l1i} J_{l3}\,,$$

$$N_i = \sum_l \frac{2l+1}{2l(l+1)}\frac{1}{k_i\Lambda_l}(D_{l1i})^2\,,$$

$$L_{ii'} = \sum_{ll'} D_{l1i} D_{l'1i'}(-1)^{l+l'+1} J_{ll'}\,, \quad \text{for } i\neq 0\,,$$

and for $i=0$ with

$$a_0 = \tfrac{12}{5} J_{22}\,,$$

$$b_0 = \tfrac{24}{7} J_{23}\,,$$

$$N_0 = \tfrac{1}{3}\,,$$

$$L_{0i'} = \sum_{l'} D_{l'1i'}(-1)^{l'+1} J_{2l'}\,.$$

As in Eqs. (48), $D_{l10} \equiv \frac{4}{3}\delta_{l,1}$.

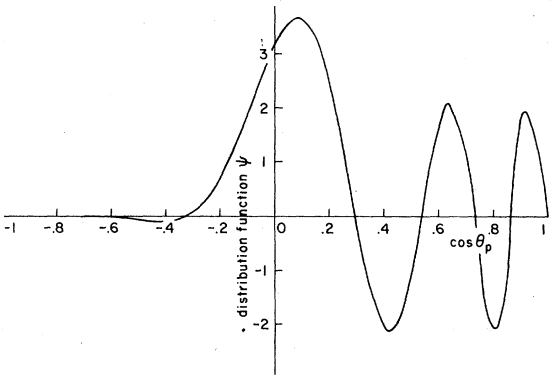

FIG. 5. Dependence of the function ψ_{1i} on $\cos\theta_p$ for the mode with $k=1558/\Lambda_2$.

In actual practice we shall retain only A_i coefficients for the same modes as appearing in the B_i expansion in a given approximation; that is, the full-range expansion Eq. (46) will also be truncated. With this expansion substituted into Eq. (43) for the complementary solution $\chi_c(z,\hat{p})$ and the effective mean free path for heat flow evaluated as in Eq. (25), we find

$$\Lambda_{\text{eff}} = \frac{5}{12}\frac{W^2}{\Lambda_2} + A_0 + \frac{3}{2}\sum_{i\neq 0}\left(\frac{1}{k_i W}A_i + O(e^{-k_i W})\right). \qquad (50)$$

It is convenient to rewrite Eq. (50) by noting each B_i amplitude and thus each A_i is the sum of a term proportional to W and one proportional to Λ_3, the two lengths in the boundary conditions. This fact may be seen from the form of Eqs. (48) and (49). Thus we can write

$$A_i = p_i W + q_i\Lambda_3\,, \quad i=1,2,\ldots\,,$$

while for the amplitude A_0 of the uniform flow mode it is more convenient to insert some numerical factors first:

$$A_0 = \tfrac{5}{2} S_1 W + 5 S_2\Lambda_3\,. \qquad (51)$$

(S_1 and S_2 will be identified later as slip coefficients). Equation (50) can then be rewritten

$$\frac{\Lambda_{\text{eff}}}{W} = \frac{5}{12}\frac{W}{\Lambda_2} + \frac{5}{2}S_1 + 5(S_2+b)\frac{\Lambda_3}{W} + c\left(\frac{\Lambda_3}{W}\right)^2 + O(e^{-kW})\,, \qquad (52)$$

with

$$b = \frac{3}{10}\sum_{i\neq 0}\frac{1}{k_i\Lambda_3}p_i\,, \quad c = \frac{3}{2}\sum_{i\neq 0}\frac{1}{k_i\Lambda_3}q_i\,.$$

The b and c terms, along with the exponential remainder, give the contributions from exponentially attenuated modes forming the boundary layers of

TABLE II. Results of various approximations used to calculate the slip coefficients S_1 and S_2 and the coefficients b and c appearing in Eq. (52).

Maximum l	No. of exponentially decaying modes	S_1	S_2	b	c
4	1	0.595	0.196	−0.0325	−0.380
6	2	0.597	0.197	−0.0316	−0.371
8	3	0.594	0.196	−0.0328	−0.376
10	4	0.595	0.196	−0.0325	−0.375
12	5	0.595	0.196	−0.0324	−0.374
14	6	0.595	0.196	−0.0324	−0.374

the nonequilibrium phonon distribution. The b term is of the same order in the mean free path as the S_2 term from the uniform flow contribution, but it turns out that the coefficient b is fairly small compared to S_2, as we shall show now.

D. Numerical results

To examine the sequence of approximations discussed above, we first fix the maximum l value and thus the number of elementary solutions retained, solve Eq. (48) numerically for the B's, then evaluate the A's and Λ_{eff} from Eqs. (49)–(52). Table II shows the results, in various approximations, for the parameters in Eq. (52). In Fig. 6 we show a plot of Λ_{eff}/W analogous to Fig. 3 for the cylindrical tube. A minimum occurs for $W/\Lambda_2 = 0.499$, which is well within the range of values of W/Λ_2 where exponential corrections to the half-space approximate treatment are very small.

V. DISCUSSION

A. Slip coefficients for phonons

It is useful to compare our results to the predictions of the Navier-Stokes equations of hydrodynamics. In this way we can extract the values of velocity slip coefficients for phonons in the two geometries. These coefficients give the hydrodynamic viscous flow velocity of the phonon gas immediately adjacent to a boundary. This flow velocity is not zero; in general, the phonon gas "slips" at a boundary as it flows along a channel, rather than sticking perfectly as is assumed in the Poiseuille flow formula [Eq. (9)].

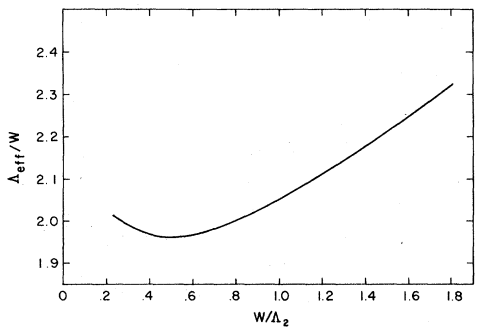

FIG. 6. Results of calculations of the effective mean free path Λ_{eff} for heat flow between two parallel plates of spacing W.

There are two uses motivating our evaluation of slip coefficients. First, they provide a quantitative way to compare our rather dissimilar calculations in the two geometries, as will be discused. More importantly, they should be useful in the experimental determination of the phonon viscosity at low temperatures. The temperature dependence of the phonon viscosity is an important experimental problem because it is such a sensitive and relatively simple probe of the dispersion relation for phonons in superfluid helium,[12] and it would be extremely useful to extend the presently available measurements of Whitworth to lower temperatures. In doing this one would want to know the range of validity of the Poiseuille formula [Eq. (9)] relating a measured heat flow to the viscosity, and when and how to include the first low-temperature corrections to the formula, which are just those due to hydrodynamic slip. Thus it is important to have reliable values of the slip coefficients for phonons.

In extracting these slip coefficients, we shall show that our calculations have the following features in the hydrodynamic limit of small viscous mean free path Λ_2.

(i) The asymptotic heat flow far from the boundary walls is as given by hydrodynamics; that is, it is described by a flow velocity field which satisfies the Navier-Stokes equations, with slip boundary conditions, including second-order slip.

(ii) Near the boundary walls there is a deviation from the hydrodynamic flow pattern which makes an additional contribution to the heat flow. This boundary-layer contribution is comparable to that from second-order slip and reduces its effect but

does not entirely eliminate it.

Regarding the first feature, it is well known in kinetic theory that the Navier-Stokes equations, in conjunction with appropriate boundary conditions, correctly describe the asymptotic parts of solutions to the Boltzmann equation. The derivation of boundary conditions for Navier-Stokes solutions has been discussed by Grad[13] for the case of gases, and we shall simply quote his result in notation suitable for the phonon problem. The relevant Navier-Stokes equation for the flow velocity $u_x(\vec{\rho})$ is the momentum-balance equation

$$\eta\nabla^2 u_x(\vec{\rho}) = S\frac{dT}{dx}; \tag{53}$$

η is the viscosity and $S(dT/dx)$ the foundation pressure gradient, Eq. (7). The boundary condition given by Grad is equivalent to

$$u_x = \Lambda_2(S_1\hat{n}\cdot\vec{\nabla})u_x - \Lambda_2\Lambda_3[S_{21}(\hat{n}\cdot\vec{\nabla})^2 + S_{22}\nabla^2 + S_{23}(\vec{\nabla}\circ\hat{n})(\hat{n}\cdot\vec{\nabla})]u_x, \tag{54}$$

which holds at each point of the boundary, with $\hat{n}$ the inward unit normal to the boundary. The S's are dimensionless coefficients, independent of geometry; S_1 is the first-order slip coefficient and the S_2's second order (Grad also finds additional second-order slip terms for more complicated flows or for geometries with varying cross section).

To verify that Eqs. (53) and (54) describe our solutions and to obtain the slip coefficients, we note that the asymptotic phonon distribution is a superposition of the particular solution of the Boltzmann equation and just the elementary solution representing uniform flow. This is because the remainder is a linear combination of spatially decaying solutions far from a boundary. Thus in either geometry we have, asymptotically,

$$\chi_{\text{asy}} = \chi_{\text{part}} + A_0\psi'$$

with χ_{part} and ψ' given by Eqs. (31) and (36) for cylindrical geometry and by (43) and (29) for plane geometry. We insert these asymptotic solutions into Eqs. (25) to calculate for each geometry the asymptotic part of the energy flux $q_x(\vec{\rho})$. With the flow velocity $u_x(\vec{\rho})$ defined by

$$q_x(\vec{\rho}) = TSu_x(\vec{\rho})$$

with S the entropy density, we then find for the asymptotic flow far from a boundary

$$u_x^{\text{asy}}(z) = -\frac{S}{\eta}\frac{dT}{dx}[\tfrac{1}{2}z(W-z) + \tfrac{1}{5}\Lambda_2 A_0^{\text{plane}}]$$

for plane geometry, and for cylindrical geometry

$$u_x^{\text{asy}}(\rho) = -\frac{S}{\eta}\frac{dT}{dx}[\tfrac{1}{4}(R^2-\rho^2) + \tfrac{1}{5}\Lambda_2 A_0^{\text{cyl}}].$$

Equations (13) and (14) have been used in obtaining these expressions from Eq. (25). One may easily verify that these velocity fields satisfy the Navier-Stokes equation (53) and boundary condition (54), if

$$A_0^{\text{plane}} = \tfrac{5}{2}S_1 W + 5(S_{21}+S_{22})\Lambda_3,$$

$$A_0^{\text{cyl}} = \tfrac{5}{2}S_1 R + \tfrac{5}{2}(S_{21}+2S_{22}+S_{23})\Lambda_3.$$

In Sec. IV we have already pointed out that A_0^{plane} can be written in precisely this form. Thus Eq. (51) and Table II from Sec. IV give slip coefficients

$$S_1 = 0.595,$$

$$S_2^{\text{plane}} \equiv S_{21}+S_{22} = 0.196.$$

Alternately, the results of our cylindrical geometry calculation for the amplitude A_0^{cyl} give

$$S_1 = 0.592,$$

$$S_2^{\text{cyl}} \equiv S_{21}+2S_{22}+S_{23} = 0.201.$$

Thus our two calculations, with quite different ways of handling the boundary conditions on the Boltzmann equation, agree to about $\frac{1}{2}\%$ for the first-order slip S_1. The second-order slips S_2^{plane} and S_2^{cyl} differ in definition by terms involving the curvature of the boundary walls and need not be the same.

These results for phonons can be compared to slip coefficients for dilute gases, which have been calculated by Cercignani and co-workers,[14] Ferziger,[15] and Sone and Yamamoto,[16] for the Bhatnagar-Gross-Krook model Boltzmann equation. In this model all mean free paths are equal in the sense that $\Lambda_2 = \Lambda_3 = \Lambda_4$, etc. This model is thus an approximate representation of the kinetics in a gas in which scattering processes of all angles occur with equal probability. In our notation,[17] the results for dilute gases are

$$S_1 = 0.4586,$$

$$S_2^{\text{plane}} = 0.1561, \quad \text{(gases)}$$

$$S_2^{\text{cyl}} = 0.8278.$$

The striking feature about these numbers in comparison with those above for phonons is that the second-order slip for dilute gases is very different in plane and in cylincrical geometry, while for phonons it is not. The near numerical equality of S_2^{plane} and S_2^{cyl} for phonons seems to be a peculiarity of the spectrum of mean free paths Λ_l obtained from Eq. (20).

Near the boundary walls there is a layer where the spatially decaying modes also contribute to the phonon distribution function. These modes decay

exponentially (plane case) or like modified Bessel functions (cylindrical case); in both cases the width of the boundary layer is of the order of $1/k_s$, where k_s is the smallest decay constant. Within the boundary layer the actual flow slows down below the hydrodynamic flow and accomodates more nearly to the stationary wall. This is shown by the velocity profile for flow in a cylinder [Fig. 4(a)]. At the wall the phonon gas does slip, though with less velocity than the hydrodynamic slip. This actual wall slip flow is carried only by those phonons headed into the boundary, since the phonons returning after being scattered from the wall have no net drift, for the diffuse boundary condition we use. Figure 4(b) shows the velocity profile in a narrower tube, $R/\Lambda_2 = 0.2$. Flow in this tube is rather far from the hydrodynamic limit in that the "boundary layer" now occupies most of the cross section and the actual flow velocity is substantially less than the hydrodynamic velocity over much of the tube.

The slowing down of the flow within the boundary layer reduces the effective mean free path Λ_{eff}. This reduction first appears in the same order in Λ_2/R or Λ_2/W as the increase due to second-order slip flow. This may be explicitly seen in our plane-geometry calculation leading to Eq. (52) and Table II. The b term in Eq. (52) is the leading boundary-layer contribution, and as seen from Table II reduces the effect of second-order slip by about 16%. In a tube the cancellation is bigger, equivalent to a 40% reduction of the second-order slip contribution. This competition between slip effects and boundary-layer effects on the total flow can be appreciated quite simply: the amplitudes A_i of the spatially decaying modes forming the boundary layer are the same order as the amplitude A_0 of the uniform flow mode carrying the hydrodynamic slip. This is true because all amplitudes are strongly coupled by the boundary conditions. The heat flux carried by these decaying modes is localized within a distance k^{-1} of the boundary walls and thus occupies only a fraction $(k^{-1})/R$ or $(k^{-1})/W$ of the cross-sectional area. Thus, integrated over the full cross section, the total flow from the boundary-layer modes is a factor $(k^{-1})/R$ or $(k^{-1})/W$ smaller than the slip flow. As these factors are proportional to Λ_3/R or Λ_3/W, the leading boundary layer contribution to the total flow is then a factor Λ_3/R or Λ_3/W smaller than the leading (first-order) slip flow. Thus it is competitive with the second-order slip.

B. Flow minimum

Both of our calculations display a minimum in the heat-flow mean free path Λ_{eff} when Λ_2 becomes comparable to the cross-section dimension R or W. The flow in the region $\Lambda_2 \lesssim R$ or $\Lambda_2 \lesssim W$ is quite complicated, and this region is really just the beginning of a very involved and gradual transition from viscous flow to, eventually, ballistic phonon propagation. Even for $\Lambda_2 \gg R$ the flow can still be far from ballistic and dominated by rapid small-angle phonon-phonon scattering with a mean free path $\Lambda_{\parallel} \ll R$; indeed this is assumed in our treatment. In this respect the situation is in contrast to the analogous case of mass flow in dilute gases, where the transition from viscous flow to free molecular streaming is much sharper.

For cylindrical tubes our calculations may be compared to the measurements of Whitworth.[5] First we shall discuss the depth of the flow minimum. As shown in Fig. 3, our calculation gives a minimum value $\Lambda_{eff}/2R$ of 0.91, i.e., 9% below the Casimir boundary-scattering value. Whitworth suggested very tentatively a deeper minimum, about 15%, for diffuse boundary scattering. His result depends somewhat on assumptions he made about how to eliminate the influence on the minimum depth of partially specular, rather than diffuse, reflection of phonons from the boundary walls. Specular reflection was evident in some degree in the region of the flow minimum in all but one of Whitworth's tubes. We do not feel there is any serious disagreement between calculation and experiment for the minimum depth.

The position of the minimum in Fig. 3 we find to be at $R/\Lambda_2 = 0.20$, which is almost twice the value for the Knudsen minimum in dilute gas flow. Whitworth however concluded that the minimum was even higher, at $R/\Lambda_2 = 0.44 \pm 0.07$. This apparent discrepancy between our calculation and experiment may not be real, for there are two major uncertainties in comparing with Whitworth's data which can only be resolved by further work. These uncertainties concern the temperature dependence of Λ_2 and the effect of phonon dispersion on other parameters than Λ_2, as we shall now discuss.

1. Effect of phonon dispersion. Whitworth converted his measurements of heat flow and temperature gradient into a temperature-dependent quantity $y(T)$ for each tube, defined by Eqs. (10) and (11) above, with the *approximations* that the specific heat C in (10) is the theoretical Debye T^3 value, and the average thermal phonon velocity $\langle v \rangle = 239$ m/sec, independent of temperature. These approximations assume no dispersion in the phonon spectrum over the energy range being probed, which at the time of Whitworth's work was believed to be true. Inclusion of phonon dispersion effects on C and $\langle v \rangle$ in Eq. (10) then raises the possibility of a temperature-dependent correction to Whit-

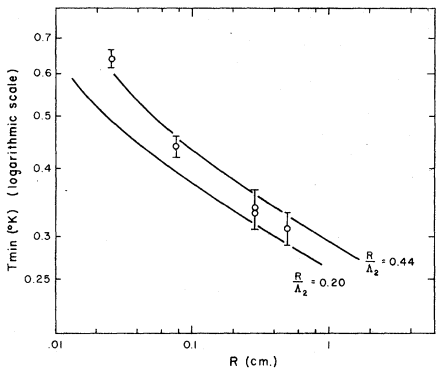

FIG. 7. Temperature of the Knudsen minimum as a function of tube radius. ○ denotes Whitworth's data. Solid lines are the temperature determined by the criteria $R/\Lambda_2 = 0.20$ and $R/\Lambda_2 = 0.44$, as indicated.

worth's $y(T)$ which could shift its minimum. We have made a very preliminary investigation of this question and find if the dispersion in the phonon energy ϵ_p is of the γp^3-type,

$$\epsilon_p = c_0(p + \gamma p^3), \quad \gamma > 0$$

then to first order in γ the minimum of $y(T)$ is shifted down to a lower temperature, where $\Lambda_2(T)$ is larger. This suggests that Whitworth has overestimated R/Λ_2 at the true minimum of $\Lambda_{eff}/2R$. We have not attempted to pursue this question, however, because in Whitworth's experiments partial specular reflection also influences the shape of the minimum, and should probably be incorporated too.

2. Temperature dependence of $\Lambda_2(T)$. From his data for tubes displaying a well-defined Poiseuille flow region of the heat flow, Whitworth determined that $\Lambda_2 \propto T^{-4.2}$ above 0.45 °K. For almost all his tubes the flow minimum occurred at a temperature below 0.45 °K, and his conclusion that $R/\Lambda_2 = 0.44$ at the minimum depends partly on an assumed extension of the $T^{-4.2}$ temperature dependence for Λ_2 down to about 0.3 °K. Current theories of $\Lambda_2(T)$, in good agreement with Whitworth's results above 0.45 °K, predict an increase faster that $T^{-4.2}$ at lower temperatures,[12] so we have felt it useful to reexamine Whitworth's data for the minimum using a theoretical expression for $\Lambda_2(T)$. In Fig. 7 are shown Whitworth's data for the temperature at the minimum of $y(T)$ in five tubes. (These data are taken from Fig. 5 of Ref. 5 without any attempt to correct the minimum position as discussed above). Also drawn for comparison are the two curves $R/\Lambda_2(T) = 0.20$, our calculated minimum position, and $R/\Lambda_2(T) = 0.44$, Whitworth's conclusion, for a theoretical $\Lambda_2(T)$ computed using the phonon dispersion relation D of Ref. 12(a). We conclude from Fig. 7 only that $R/\Lambda_2 = 0.20$ is not flatly ruled out by the data.

Further experimental work would be very useful. For the investigation of the minimum, the ideal measurement would be of flow versus tube radius at constant temperature, but this does, of course, involve considerable work. It would be valuable, though, to have measurements over a wide enough range of tube radii so that some large-radius tubes feature hydrodynamic Poiseuille, or Poiseuille-plus-slip flow (thus permitting easy determination of Λ_2) at the same temperature that other smaller-radius tubes have flow minima. This would allow a direct experimental determination of R/Λ_2 at the minimum.

ACKNOWLEDGMENT

This work was supported in part by the NSF through the Materials Research Laboratory at Brown University and through Grant No. DMR 77-12249.

*Permanent address: Dept. of Physics, Arizona State Univ., Tempe, Ariz. 85281.

[1]For a review, see J. Wilks, *The Properties of Liquid and Solid Helium* (Oxford University, London, 1967).
[2]H. J. Maris, Rev. Mod. Phys. 49, 341 (1977).
[3]H. J. Maris, Phys. Rev. Lett. 30, 312 (1973); Phys. Rev. A 9, 1412 (1974).
[4]W. M. Saslow, Phys. Rev. A 10, 2482 (1974).
[5]R. W. Whitworth, Proc. R. Soc. A 246, 390 (1958).
[6]H. B. G. Casimir, Physica (Utr.) 5, 595 (1938).
[7]Note that this differs from the mean free path Λ_{theor} defined in Ref. 12 by a factor of $\frac{5}{3}$.
[8]M. Knudsen, Ann. Phys. (Paris) 28, 75 (1909).
[9]S. Simons. Proc. R. Soc. Lond. A 315, 239 (1970).
[10]This form of the relaxation rate spectrum also describes small-angle phonon scattering in a weakly interacting Bose gas; see S.-K. Ma, J. Math. Phys. 12, 2157 (1971).
[11]Compare the related discussion by S. Simons, Proc. R. Soc. A 301, 387, 401 (1967).
[12](a) H. J. Maris, Phys. Rev. A 8, 1980 (1973). (b) D. Benin, Phys. Rev. B 11, 145 (1975). (c) V. L. Gurevich and B. D. Laikhtman, Zh. Eksp. Teor. Fiz. 69, 1230 (1975) [Sov. Phys.-JETP 42, 628 (1976)].
[13]H. Grad, in *Transport Theory* (SIAM-AMS Proceedings, Vol. 1) (American Mathematical Society, Providence, Rhode Island, 1969), Vol. 1, pp. 291 ff.
[14]C. Cercignani, *Mathematical Methods in Kinetic Theory* (Plenum, New York, 1969), Chap. VII.
[15]J. H. Ferziger, Phys. Fluids 10, 1448 (1967).
[16]Y. Sone and K. Yamamoto, Phys. Fluids 11, 1672 (1968).

[17] The slip coefficients are defined by terms in the boundary condition Eq. (54), which also involves in mean free path Λ_2. For purposes of comparison we have defined Λ_2 for a gas from the viscosity relation $\eta = \frac{1}{5} \rho \langle v \rangle \Lambda_2$, with ρ the mass density and $\langle v \rangle$ the mean particle speed. This is not the definition of the mean free path used in Refs. 14–16.